



Published in final edited form as:

Cancer Res. 2010 April 15; 70(8): 3071–3079. doi:10.1158/0008-5472.CAN-09-2877.

The Connectivity Map links Iron Response Protein-1 (IRP1)-mediated inhibition of HIF2a translation to the anti-inflammatory 15-deoxy- $\Delta^{12,14}$ -Prostaglandin J₂

Michael Zimmer¹, Justin Lamb², Benjamin L. Ebert^{2,3}, Mary Lynch⁴, Christopher Neil¹, Emmett Schmidt⁴, Todd R. Golub², and Othon Iliopoulos¹

¹ Center for Cancer Research, Massachusetts General Hospital Cancer Center, Charlestown, MA and the Department of Medicine, Hematology-Oncology Unit, Massachusetts General Hospital, Boston, MA

² The Broad Institute of Harvard University and Massachusetts Institute of Technology, Cambridge, MA

³ Harvard Stem Cell Institute, Brigham and Women's Hospital, Boston, MA

⁴ The Pediatric Service, Massachusetts General Hospital and the Massachusetts General Hospital Cancer Center, Boston, MA

Abstract

Hypoxia Inducible Factors 1 and 2 (HIF1 and HIF2) are heterodimeric transcription factors consisting of alpha regulatory subunits and a constitutively expressed beta subunit. The expression of alpha regulatory subunits is promoted by hypoxia, cancer-associated mutations and inflammatory cytokines. Thus, HIF1 and HIF2 provide a molecular link between cancer and inflammation. We have recently identified novel small molecules that selectively inhibit translation of the HIF2a message and thereby powerfully inhibit the expression of HIF2a target genes. We report here that Connectivity Map analysis links three of these compounds to the anti-inflammatory cytokine 15-deoxy- $\Delta^{12,14}$ -Prostaglandin J₂ (PGJ₂). As with our identified compounds, PGJ₂ inhibits translation of the HIF2a message in an mTOR independent manner by promoting the binding of Iron Regulatory Protein-1 (IRP1) to a non-canonical Iron Responsive Element (IRE) embedded within the 5'-UTR of the HIF2a message. The IRE is necessary and sufficient for mediating the effect. Mutation of the IRE sequence, or down regulation of IRP1 expression, blocks the effect of PGJ₂ on HIF2a translation. This is the first report of an endogenous natural molecule regulating HIF2a translation and it suggests that part of the anti-inflammatory and putative anti-neoplastic effects of PGJ₂ may be mediated through inhibition of HIF2a within tumor epithelial cells themselves and/or mesenchymal cells of the tumor microenvironment.

Keywords

Renal Cancer; hypoxia; prostaglandin; angiogenesis; iron

INTRODUCTION

Hypoxia Inducible Factor (HIF) is directly linked to cancer progression, angiogenesis and inflammation. HIF is critical for the transcriptional regulation of the cellular response to hypoxia. In addition to hypoxia, tumor associated mutations that activate the PI3K pathway, inactivate the von Hippel-Lindau (VHL) gene, or disrupt the mitochondrial Krebs cycle result in increased HIF activity (1). HIF is upregulated in the majority of human tumors and it has been proposed as a prognostic factor for aggressive disease. Many preclinical models indicate that HIF inactivation may lead to suppression of tumor growth (2–4) as well as regression of pathologic angiogenesis in non-malignant diseases such as macular regeneration (5).

HIF has also been implicated in promoting inflammatory responses. Targeted deletion of HIF1 α from macrophages of transgenic mice led to significant attenuation of experimentally induced serum sickness or chemically induced dermatitis (6). Recently, HIF1 α has been identified as a direct transcriptional target of NF κ B (7). It is therefore not surprising that HIF has been proposed, and to a great extent validated, as a therapeutic molecular target for anti-neoplastic and anti-inflammatory interventions (8).

In an effort to discover HIF-based anti-neoplastic and anti-inflammatory compounds, we conducted a cell-based screen and discovered four small molecules that decrease HIF2 α expression under conditions of normoxia and hypoxia (9). Microarray analyses indicated that these small molecules powerfully inhibited the expression of signature HIF2 α target genes. As part of our studies to understand the mechanism of action of these inhibitors, we utilized the Connectivity Map to identify other small molecules that might mimic the gene expression changes induced by the HIF2 α inhibitors. The Connectivity Map is a reference collection of gene-expression profiles from cultured human cell lines (breast cancer epithelial cell line MCF7, prostate cancer cells PC3, the non-epithelial leukemia line HL60 and the melanoma cell line SKMEL5) treated with a large number of diverse bioactive small molecules. The current collection (build 02) contains data for 6,100 treatment instances representing 1,309 discrete small molecules. Comparative analysis between a “query” gene expression signature (generated by profiling cells treated with small molecules or corresponding to a physiologic or a disease specific process) and the Connectivity Map collection may highlight similar patterns of gene-expression changes and therefore lead to the discovery of functional connections between drugs, genes and diseases. In the case of our HIF2 α inhibitor “query” signatures, the connectivity analysis strongly linked the activity of three of our four inhibitors to the endogenous anti-inflammatory 15-deoxy- $\Delta^{12,14}$ -Prostaglandin J₂ (PGJ₂).

In this manuscript we confirm this linkage experimentally and we show that PGJ₂ inhibits HIF2 α translation in an mTOR-independent manner. It acts by enhancing the binding of the Iron Regulatory Protein-1 (IRP1) to the recently identified Iron Responsive Element (IRE) located within the 5'-UTR of HIF2 α message (9,10). Mutational analyses and reporter hybrid experiments indicate that the IRE element is both necessary and sufficient for the ability of PGJ₂ to inhibit HIF2 α translation. There is a growing body of evidence suggesting that PGJ₂ is a key endogenous negative regulator of inflammation and angiogenesis (11) and that it constitutes one of the mechanisms employed by cells to resolve the inflammatory response (12–14). We therefore propose that HIF2 is likely an important target through which PGJ₂ exerts its anti-inflammatory and anti-proliferative effects and that this interaction is one of the endogenous mechanisms by which cells restore HIF2 α levels upon restoration of normal ambient oxygen tension.

MATERIALS AND METHODS

Plasmids, cell culture conditions and luciferase assays

Complete description of plasmids and cell lines used in this study is provided elsewhere (9). Buffers were made as described in Molecular Cloning (15) and chemicals ordered through Sigma. Cells were grown on DMEM-10% Fetal Clone and transfected with Lipofectamine 2000. Unless stated differently, 25% confluent cells were treated with either fresh DMEM medium, DMEM supplemented with DMSO-only or PGJ₂ for 24 hours and then changed into fresh DMEM medium, DMEM supplemented with DMSO-only or PGJ₂ for an additional 24 hours, before harvesting at 90–100% confluence. For hypoxic experiments, cells were incubated at the indicated oxygen concentration for the latter 24 hours. All cell lines used in this work were purchased from ATCC, aliquoted, immediately frozen, and re-plated for the purposes of these experiments within the last 9 months. Luciferase assays were performed using the Luciferase Assay Reporter System (Promega, E1910). Stable clones were normalized to medium only treated wells.

Gene-expression and Connectivity Map Analysis

Gene-expression profiles of 786-0 cells, treated with small-molecule inhibitors or vehicle control, were generated using Affymetrix U133 Plus 2.0 microarrays and compound signatures were derived as described elsewhere (9). Raw gene-expression data have GEO series accession number GSE13818. Compound signatures from which non-HG-U133A probe sets were removed (Supplementary Table 1) were used to query the Connectivity Map (build 02). Details of the Connectivity Map dataset and analytics are provided elsewhere (16).

Western blots

Proteins were immunoblotted as described before (4). Primary antibodies (1:1000) include anti-HIF2a (Novus, NB100-132), anti-HIF2a (NB100-122), anti-Glut-1 (Alpha Diagnostics, GT-11-A), anti-p70S6K (Cell Signaling Technologies, CST 9202), anti-phospho T389 p70S6K (CST 9205S), anti-phospho S235/6 S6 (CST 2211S), anti-RhoB (CST 2098S), or anti-Actin (Novus, ab8226). Gel densitometry was performed using SynGene Gene Tools software package (Synoptics, Ltd).

Cycloheximide experiments

10 µg/mL cycloheximide (CHx) was added to DMSO or PGJ₂ treated cells at t = -4, -3, -2, and -1 hours and cells were lysed at t = 0. HIF2a expression was quantified by western blot.

Quantitative real time polymerase chain reaction (qRT-PCR)

The following intron-spanning primers were used (forward and reverse correspondingly): for beta-2-microglobulin (B2M) 5'-TTTCATCCATCCGACATTGA-3' and 5'-ATCTTCAAACCTCCATGATG-3'; for HIF2a 5'-GGATCAGCGCACAGAGTTC-3' and 5'-GTACTGGGTGGCGTAGCACT-3'; for EGLN3 5'-ATCAGCTTCCTCCTGTCCCT-3' and 5'-GGGCTGCACTTCGTGTGGGT-3'. Nascent HIF2a message levels were determined using intronic primers 5'-AGACGGTGGACTCCGCCA-3' and 5'-TTAAAGGGAGGGGTACAC-3'.

In vivo ³⁵S-methionine pulse-label experiments

Cells were treated with medium only, DMSO, or PGJ₂, pulsed with ³⁵S-Methionine (NEN) for 30 minutes and chased with 3 mg/mL methionine for 1.5 and 3 hours. 500 µg cell lysate was immunoprecipitated with 2 µg anti-HIF2a (NB100-122) or control anti-HA Y-11 (Santa Cruz, sc-805) antibodies.

Other assays

Polysomal profile analysis (17), Electrophoretic Mobility Shift Assays (EMSAs) and in vitro iron competition assays (9), were performed as described. Prostaglandin D₂-MOX EIA Kit (Cayman Chemical Company, 212011) was used for PGD₂ ELISA (18).

RESULTS

Connectivity Map analysis links HIF2a inhibitors to PGJ₂

In previous work we described how we identified several small molecule HIF2a inhibitors (9). To gain insight into the signaling pathways perturbed by these inhibitors, we generated gene expression signatures for these compounds in the human renal cell carcinoma (RCC) cell line 786-O and subjected these signatures to Connectivity Map analysis. 786-O cells are VHL-deficient cells and therefore constitutively expressed HIF2a. Comparison of gene expression changes induced by the small molecule HIF2a inhibitors to the profiles included in the Connectivity Map database strongly suggested that three out of four compounds (40,41 and 76) shared a functional similarity with the anti-inflammatory PGJ₂ (Figure 1a).

PGJ₂ decreases HIF2a activity in a dose-dependent manner

To validate the Connectivity Map-derived prediction that PGJ₂ is involved in HIF signaling, we treated 786-O derived HRE-luciferase expressing (7H4) and SV40-luciferase expressing (7SV) control cells with increasing doses of PGJ₂. Fresh medium containing the indicated concentrations of PGJ₂ or vehicle-only DMSO control was applied to cells at 24-hour intervals. Luciferase activity was measured at 48 hours. PGJ₂ decreased HRE-driven luciferase activity (Figure 1b) in a dose dependent manner, with an IC_{50,app} of 5 μM, while SV40-driven luciferase activity was not affected. This action of PGJ₂ appears to be independent of NFκB activation. Application of IKK inhibitor BMS-345541 did not alter the HRE-luciferase activity in 786-O cells (Figure S1a and b). Moreover, this appears also to be a PPAR-gamma-independent function of PGJ₂; the PGJ₂/HIF inhibitor linkage holds strong even in Connectivity Map comparisons using expression profiles obtained from PPAR-gamma negative cells (MCF7) and application of a PPAR-gamma inhibitor, GW9662, did not block the effect of PGJ₂ on HIF2a activity (data not shown). This decrease in HRE-mediated luciferase activity closely matched the decrease in HIF2a protein expression as well as that of the HIF2a target genes Glut-1, as measured by Western blot, and EGLN3, as measured by qRT-PCR (Figure 1c). To investigate whether the effect of PGJ₂ on HIF2a protein expression is due to decreased transcription of the HIF2a gene, we performed qRT-PCR to examine HIF2a mRNA expression in PGJ₂ or vehicle-only DMSO treated 786-O cells. We observed no concomitant decrease in HIF2a mRNA expression, indicating that the transcription of HIF2a mRNA was not affected (Figure 1d). To investigate whether PGJ₂ alters the stability of HIF2a protein, we examined the half-life of HIF2a in PGJ₂ or vehicle-only DMSO treated 786-O cells following the addition of cycloheximide. These results show no indication that PGJ₂ affects HIF2a protein half-life (Figure S2a and b).

The effect of PGJ₂ on HIF2a expression and activity is not a cell line specific phenomenon; treatment of several VHL-deficient human RCC lines with PGJ₂ similarly resulted in decreased HIF2a protein expression (Figure S3a). Moreover, consistent with the fact that the HIF1a candidate IRE sequence appears to be non functional (9), at least in the cell lines tested, we see no decrease in HIF1a expression in UMRC2 cells treated with PGJ₂ (Figure S3b).

PGJ₂ inhibits HIF translation in an mTOR-independent manner

To determine if PGJ₂ decreases translation of the HIF2a message, we evaluated the synthesis rate and stability of the newly synthesized HIF2a by an ³⁵S-methionine pulse chase experiment

on PGJ₂ or vehicle only DMSO treated 786-O cells. PGJ₂ was found to significantly decrease the amount of protein translated from the mRNA without decreasing the half-life of the protein (Figure 2a, upper panel). Loading control is 1/1000th of the cell lysate used in the respective immunoprecipitation directly loaded into an SDS-PAGE gel. This loading control demonstrates not only that equal protein was used in each immunoprecipitation but also that PGJ₂ does not globally decrease cellular translation (Figure 2a, lower panel). Consistent with the interpretation that PGJ₂ does not affect global translation, polysome analysis was performed on vehicle-only DMSO, rapamycin or PGJ₂ treated 786-O. These experiments show that PGJ₂ had little effect on the number of ribosomes actively engaged in translation while rapamycin attenuated it. However, PGJ₂, like rapamycin, did appear to slightly decrease the monosome fraction (Figure 2b).

It has been shown before that mTOR inhibits HIF translation as part of a global effect on translation (9,19–21). We therefore examined whether the effect of PGJ₂ on HIF2a translation could be attributed to inhibition of mTOR activity. 786-O cells were treated with medium only, DMSO (vehicle only), rapamycin or PGJ₂ and the effect of these treatments on mTOR activity was monitored by detecting phospho-S6, p70S6K and phospho-p70S6K levels, as measured by Western blot using total or phospho-specific antibodies. HIF2a protein expression and HRE activity were decreased by both PGJ₂ and rapamycin. However, only rapamycin decreased phosphorylation of the downstream mTOR targets p70S6K and rpS6 (Figure 2c).

The 5'-UTR of HIF2a mRNA is necessary and sufficient for the inhibitory effect of PGJ₂

Since PGJ₂ inhibits translation of the HIF2a message in an mTOR independent manner, we next examined whether the 5'-UTR of the HIF2a message might be involved in mediating its effect. We therefore generated two luciferase reporter constructs, the first driven by the endogenous HIF2a promoter alone (HIF) and the second driven by the HIF2a promoter containing the 5'-UTR (HIF-UTR). These constructs were stably transfected into 786-O cells. Treatment with PGJ₂ decreased the luciferase activity derived from the UTR-containing plasmid but not the plasmid driven by the HIF promoter alone. Moreover, this effect was equal in magnitude to the effect on HRE-driven reporter activity. The ratio of normalized HRE-luciferase over SV40-luciferase reporter activities is shown compared to the ratio of normalized HIF-UTR-luciferase over HIF-luciferase activities in vehicle only DMSO versus PGJ₂ treated cells (Figure 2d, upper panel). These experiments indicate that HIF2a 5'-UTR is necessary for the inhibitory effect of PGJ₂ on HIF2a translation, and corroborate the qRT-PCR findings that the effect of PGJ₂ on HIF is not transcriptional.

We next wanted to test if the HIF2a 5'-UTR is sufficient for conferring sensitivity to PGJ₂. To test this generated a luciferase reporter construct (SV-UTR) in which the entire 488 base pair HIF2a 5'-UTR was cloned between the SV40 promoter and the luciferase gene of the same SV40-luciferase reporter (SV) used as a HIF/hypoxia-independent control in the previously discussed experiments. We compared this set of luciferase reporters to second matched set, consisting of a CMV-luciferase reporter by itself and the same CMV-luciferase into which a synthetic stem loop was cloned between the CMV promoter and the start of the luciferase gene (CMV-SL; kind gifts of Michele Pagano). This luciferase reporter set serves as a random 5'-UTR control that might capture possible effects on RNA helicase activity (22). Shown are the ratios of normalized CMV-SL over CMV and SV-UTR over SV luciferase reporter activities from vehicle only DMSO versus PGJ₂ treated cells. The results indicate that the effect of PGJ₂ that is mediated through the HIF2a 5'-UTR element is indeed heterologously transferable to a different promoter element, whereas PGJ₂ had no effect on the synthetic 5'-UTR element (Figure 2d, lower panel).

The Iron Responsive Element (IRE) within the HIF2a 5'-UTR is responsible for the effect of PGJ₂ on HIF translation

To map the domain responsible for mediating the effect of PGJ₂ on translation of the HIF2a message, we created several reporter constructs in which different segments of the HIF2a 5'-UTR were cloned between the HIF2a promoter and the start of the luciferase gene and used these constructs to generate stable 786-O derived cell lines. These lines were then treated with vehicle-only DMSO or PGJ₂. We found that the effect of PGJ₂ maps to a 50 base pair segment of the 5'-UTR that contains a recently reported Iron Responsive Element (IRE) (9). A mutation in the IRE consensus loop completely abolished PGJ₂ sensitivity. These results are summarized in Figure 3a, where the normalized ratio of luciferase activities from PGJ₂ over vehicle-only DMSO treated cells is shown.

Iron Regulatory Protein-1 (IRP1) is necessary for the effect of PGJ₂ on HIF2a

The IREs are the mRNA target sequences for the binding of both Iron Regulatory Proteins IRP1 and IRP2 (23). Nevertheless, slight variations in the IRE sequences can result in higher affinity for one of the two proteins (24). We showed before that it is mainly the IRP1 and not IRP2 that can measurably bound to the HIF2a IRE element, under normoxic conditions, when expressed in endogenous levels (9). We therefore examined whether IRP1 and/or IRP2 is required for the effect of PGJ₂ on HIF2a by assessing the expression of the HIF2a target gene EGLN3 in 786-O derived lines infected with shRNAs targeting IRP1, IRP2 or both IRP1 and IRP2 concomitantly (Figure 3b). In keeping with our previous observation that HIF2a IRE translation is primarily repressed through IRP1, knocking down the expression of IRP1 resulted in increased activity of HIF2a, consistent with the observation that IRP1 represses HIF2a translation (Figure 3b). More importantly, down regulation of IRP1 abolished the ability of PGJ₂ to repress HIF2a activity, while inactivation of IRP2 did not (Figure 3b). These findings are consistent with the model by which PGJ₂ represses HIF2a translation by enhancing endogenous IRP1 mRNA binding activity.

PGJ₂ directly enhances the binding of IRP1 to the HIF2a IRE

We therefore next sought to determine if PGJ₂ affects the expression of IRP1 and/or IRP2 and we found that, as is the case for the 3 small molecule HIF inhibitors that linked to PGJ₂ in the Connectivity Map, IRP1 expression is not affected by PGJ₂ treatment while IRP2 expression is minimally increased (data not shown). However, IRP2 contributes very little—if at all—to the total IRP bound to the HIF2a IRE (9). We therefore hypothesized that the effect of PGJ₂ on HIF2a IRE is due to the enhanced binding of IRP1.

To examine this latter possibility, we performed an electrophoretic mobility shift assay (EMSA) using a radiolabeled wild type or mutant IRE probe to determine if IRP1 binding is increased in PGJ₂ treated cells (Figure 4a). We found that pre-treatment of cells with PGJ₂ increased the specific IRE binding activity of cell lysates under conditions in normoxia. This shifted band can be supershifted with IRP1 but not IRP2 antibodies (data not shown). The effect of PGJ₂ on IRP1 binding to the HIF2a IRE probe under 1% oxygen was very subtle but appeared to be consistently present. Given the scant effect of PGJ₂ on enhancing IRP1 binding in hypoxia, as measured by EMSA, we decided to further examine the ability of PGJ₂ to decrease HIF2a activity at various concentrations of ambient oxygen that correspond to physiologic or extreme conditions of tissue oxygenation. The results indicate that PGJ₂ clearly has the ability to repress HIF2a activity at a wide range of oxygen concentrations spanning the range of physiologic tissue oxygenation (Figure 4b). Rapamycin, which decreases HIF2a activity and expression (Figure 5a and b), does not affect IRP1 binding to the HIF2a IRE (Figure 5c). Instead, it decreases HIF2a transcription (Figure 5d), as reported before (25).

DISCUSSION

Connectivity Mapping linked the gene expression signature of small molecule HIF2a inhibitors to the molecular signature of PGJ₂. Here we experimentally validate this hypothesis and we show that this function of PGJ₂ is mediated through enhanced IRP1 binding to the HIF2a IRE. This is the first report of an endogenous cellular metabolite that regulates HIF2a translation through the IRE mechanism.

Activation of the arachidonic acid (AA) cascade generates prostaglandin H₂ (PGH₂) through the activity of cyclooxygenase synthases. PGH₂ can be further metabolized to prostaglandin E₂ (PGE₂) or PGD₂, through corresponding synthases. PGJ₂ is a non-enzymatic degradation product of PGD₂. PGE₂, in contrast to PGJ₂, has the ability to promote HIF1a activity (26,27), through activation of the EGFR-Src-ERK signaling pathways (28,29). In addition, PGE₂ promotes colonic adenomatous polyposis through PPAR-delta activation (30, 31). It therefore appears that PGE₂ promotes the “pro-inflammatory” and “pro-proliferative” effects of the AA cascade. In contrast, PGJ₂ inhibits HIF2a translation and activity. Although PGJ₂ has recently been reported to stabilize HIF1a, through inhibition of a lysosomal degradation pathway (32), we see no such effect in PGJ₂ treated UMRC2 cells. It appears that PGJ₂ may “oppose” the effects of PGE₂, and therefore may be a key determinant of the final outcome of AA signaling.

One possibility to explain the link between HIF2a inhibitors and PGJ₂ is that the former increase the endogenous expression of PGJ₂, a non-enzymatic degradation product of PGD₂. The latter is made from PGH₂ by lipocalin or hematopoietic PGD₂ synthases. Neither the addition of the Cox-1/2 inhibitors Indomethacin and Sulindac nor the hematopoietic PGD₂ synthase inhibitor HQL-79 had any effect on the activity of the compounds (Figure S4a). Similarly, these pharmacological manipulations had no effect of baseline HIF2a expression in 786-O cells (data not shown). We were unable to detect PGD₂ in compound treated 786-O cell supernatants directly, using a commercially available ELISA kit (data not shown). However, we found that PGJ₂ and all compounds increased the expression of RhoB, an endogenous PPAR-gamma target gene (Figure S4b,c) (33). Taken together, these data suggest, but clearly do not prove, that the compounds may serve, directly or indirectly, as PGJ₂ mimetics. Future experiments, involving direct measurement of PGD₂ and PGJ₂ by mass spectrometry as well as cells generated from PGD₂ synthase knock out mice, should answer definitely the relation between HIF2a inhibitors and endogenous PGJ₂.

An analysis of the Oncomine database shows that the expression of IRP1 and lipocalin type PDGS is down-regulated in kidney cancer. Specifically, 3 of 17 analyses (2 of 7 data sets) showed decreased IRP1 expression in tumor versus normal with a p-value of <0.0001. Similarly, 3 of 14 analyses (2 of 6 data sets) showed decreased lipocalin PGDS expression, also with a p-value <0.0001. These data suggest that there may be selective pressure in RCC to reduce the activity of IRP1. Of relevant interest are also the observations that constitutional deletion of hematopoietic PGD synthase promotes colonic polyposis in APC^{+/-} mice (34).

PGJ₂ has been reported to inhibit global translation of cellular proteins through binding to and inactivation of eIF4A and sequestration of TRAF2 into stress granules (35). In our work we employed lower concentrations of PGJ₂ that did not affect global translation. It is likely that the first response of cells to moderate levels of PGJ₂ concentrations is to selectively down-regulate HIF2a translation, while higher doses may be associated with a global reduction of protein translation.

Up regulation of IRP1 binding activity by PGJ₂ is likely to promote iron uptake and availability in sites of inflammation. Iron is essential for oxidative burst of PMNs and macrophages, and is therefore important for maintenance of the local inflammatory and immune responses (36,

37). The availability of PGJ₂ may be a mechanism by which the end of inflammatory phase (by inhibiting translation of the HIF2a message) is linked to restoration of iron stores in resident inflammatory and immune cells.

In cells, the majority of IRP1 functions as a cytosolic aconitase. Reduction of cellular iron stores causes a conformational change in the iron-sulfur cluster (ISC) of IRP1 protein that concomitantly decreases its aconitase activity and promotes its binding to IREs (38). Our data indicate that changes in the intracellular levels of PGJ₂ promote the RNA binding activity of IRP1. The exact mechanism by which PGJ₂ signals to IRP1 will be the object of further studies. Currently, we have shown that PGJ₂ does not act as an iron chelator and therefore it is likely to affect IRP1 through a novel, ISC-dependent or independent mechanism (Figure S5).

In summary, we provide evidence for a novel connection between cancer and inflammation in which programs involved in the resolution of inflammation may modify tumor vascularization. This connection may contribute to new strategies of cancer chemoprevention.

Supplementary Material

Refer to Web version on PubMed Central for supplementary material.

Acknowledgments

We thank M. Pagano for the pCMV and pCMV-SL constructs and N. Dyson and J. Settleman for their comments on the manuscript. Supported by the NIH 5R01CA104574 and the MGH Bertucci Center for Genitourinary Oncology Award (OI), the VHL Family Alliance and the DF/HCC Kidney Cancer Program Career Development Awards (MZ) and the NIH Genomics Based Drug Discovery—Target ID Project Grant RL1HG004671, administratively linked to NIH RL1CA133834, RL1GM084437, and UL1RR024924 (JL, TRG).

References

1. Iliopoulos O. Molecular biology of renal cell cancer and the identification of therapeutic targets. *J Clin Oncol* 2006;24:5593–600. [PubMed: 17158545]
2. Kondo K, Klco J, Nakamura E, Lechpammer M, Kaelin WG. Inhibition of HIF is necessary for tumor suppression by the von Hippel-Lindau protein. *Cancer Cell* 2002;1:237–46. [PubMed: 12086860]
3. Kondo K, Kim WY, Lechpammer M, Kaelin WG. Inhibition of HIF2alpha Is Sufficient to Suppress pVHL-Defective Tumor Growth. *PLoS Biol* 2003;1:83.
4. Zimmer M, Doucette D, Siddiqui N, Iliopoulos O. Inhibition of hypoxia-inducible factor is sufficient for growth suppression of VHL^{-/-} tumors. *Mol Cancer Res* 2004;2:89–95. [PubMed: 14985465]
5. Zhang P, Wang Y, Hui Y, et al. Inhibition of VEGF expression by targeting HIF-1 alpha with small interference RNA in human RPE cells. *Ophthalmologica* 2007;221:411–7. [PubMed: 17947829]
6. Cramer T, Yamanishi Y, Clausen BE, et al. HIF-1alpha is essential for myeloid cell-mediated inflammation. *Cell* 2003;112:645–57. [PubMed: 12628185]
7. Rius J, Guma M, Schachtrup C, et al. NF-kappaB links innate immunity to the hypoxic response through transcriptional regulation of HIF-1alpha. *Nature* 2008;453:807–11. [PubMed: 18432192]
8. Giaccia A, Siim BG, Johnson RS. HIF-1 as a target for drug development. *Nat Rev Drug Discov* 2003;2:803–11. [PubMed: 14526383]
9. Zimmer M, Ebert BL, Neil C, et al. Small-molecule inhibitors of HIF-2a translation link its 5'UTR iron-responsive element to oxygen sensing. *Mol Cell* 2008;32:838–48. [PubMed: 19111663]
10. Sanchez M, Galy B, Muckenthaler MU, Hentze MW. Iron-regulatory proteins limit hypoxia-inducible factor-2alpha expression in iron deficiency. *Nat Struct Mol Biol* 2007;14:420–6. [PubMed: 17417656]
11. Kim EH, Surh YJ. 15-deoxy-Delta12,14-prostaglandin J2 as a potential endogenous regulator of redox-sensitive transcription factors. *Biochem Pharmacol* 2006;72:1516–28. [PubMed: 16987499]

12. Rajakariar R, Hilliard M, Lawrence T, et al. Hematopoietic prostaglandin D2 synthase controls the onset and resolution of acute inflammation through PGD2 and 15-deoxyDelta12,14-PGJ2. *Proc Natl Acad Sci U S A* 2007;104:20979–84. [PubMed: 18077391]
13. Gilroy DW, Colville-Nash PR, McMaster S, Sawatzky DA, Willoughby DA, Lawrence T. Inducible cyclooxygenase-derived 15-deoxy(Delta)12-14PGJ2 brings about acute inflammatory resolution in rat pleurisy by inducing neutrophil and macrophage apoptosis. *Faseb J* 2003;17:2269–71. [PubMed: 14563690]
14. Bell-Parikh LC, Ide T, Lawson JA, McNamara P, Reilly M, FitzGerald GA. Biosynthesis of 15-deoxy-delta12,14-PGJ2 and the ligation of PPARgamma. *J Clin Invest* 2003;112:945–55. [PubMed: 12975479]
15. Sambrook; Fritsch; Maniatis, editors. *Molecular Cloning: a Laboratory Manual*. CSHL Press; 1989.
16. Lamb J, Crawford ED, Peck D, et al. The Connectivity Map: using gene-expression signatures to connect small molecules, genes, and disease. *Science* 2006;313:1929–35. [PubMed: 17008526]
17. Lynch M, Chen L, Ravitz MJ, et al. hnRNP K binds a core polypyrimidine element in the eukaryotic translation initiation factor 4E (eIF4E) promoter, and its regulation of eIF4E contributes to neoplastic transformation. *Mol Cell Biol* 2005;25:6436–53. [PubMed: 16024782]
18. Wang J, Buss JL, Chen G, Ponka P, Pantopoulos K. The prolyl 4-hydroxylase inhibitor ethyl-3,4-dihydroxybenzoate generates effective iron deficiency in cultured cells. *FEBS Lett* 2002;529:309–12. [PubMed: 12372619]
19. Hudson CC, Liu M, Chiang GG, et al. Regulation of hypoxia-inducible factor 1alpha expression and function by the mammalian target of rapamycin. *Mol Cell Biol* 2002;22:7004–14. [PubMed: 12242281]
20. Majumder PK, Febbo PG, Bikoff R, et al. mTOR inhibition reverses Akt-dependent prostate intraepithelial neoplasia through regulation of apoptotic and HIF-1-dependent pathways. *Nat Med* 2004;10:594–601. [PubMed: 15156201]
21. Brugarolas J, Lei K, Hurley RL, et al. Regulation of mTOR function in response to hypoxia by REDD1 and the TSC1/TSC2 tumor suppressor complex. *Genes Dev* 2004;18:2893–904. [PubMed: 15545625]
22. Yang HS, Cho MH, Zakowicz H, Hegamyer G, Sonenberg N, Colburn NH. A novel function of the MA-3 domains in transformation and translation suppressor Pcd4 is essential for its binding to eukaryotic translation initiation factor 4A. *Mol Cell Biol* 2004;24:3894–906. [PubMed: 15082783]
23. Rouault TA. The role of iron regulatory proteins in mammalian iron homeostasis and disease. *Nat Chem Biol* 2006;2:406–14. [PubMed: 16850017]
24. Ke Y, Wu J, Leibold EA, Walden WE, Theil EC. Loops and bulge/loops in iron-responsive element isoforms influence iron regulatory protein binding. Fine-tuning of mRNA regulation? *J Biol Chem* 1998;273:23637–40. [PubMed: 9726965]
25. Toschi A, Lee E, Gadir N, Ohh M, Foster DA. Differential dependence of hypoxia-inducible factors 1 alpha and 2 alpha on mTORC1 and mTORC2. *J Biol Chem* 2008;283:34495–9. [PubMed: 18945681]
26. Liu XH, Kirschenbaum A, Lu M, et al. Prostaglandin E2 induces hypoxia-inducible factor-1alpha stabilization and nuclear localization in a human prostate cancer cell line. *J Biol Chem* 2002;277:50081–6. [PubMed: 12401798]
27. Fukuda R, Kelly B, Semenza GL. Vascular endothelial growth factor gene expression in colon cancer cells exposed to prostaglandin E2 is mediated by hypoxia-inducible factor 1. *Cancer Res* 2003;63:2330–4. [PubMed: 12727858]
28. Pai R, Soreghan B, Szabo IL, Pavelka M, Baatar D, Tarnawski AS. Prostaglandin E2 transactivates EGF receptor: a novel mechanism for promoting colon cancer growth and gastrointestinal hypertrophy. *Nat Med* 2002;8:289–93. [PubMed: 11875501]
29. Wang D, Buchanan FG, Wang H, Dey SK, DuBois RN. Prostaglandin E2 enhances intestinal adenoma growth via activation of the Ras-mitogen-activated protein kinase cascade. *Cancer Res* 2005;65:1822–9. [PubMed: 15753380]
30. Wang D, Wang H, Shi Q, et al. Prostaglandin E(2) promotes colorectal adenoma growth via transactivation of the nuclear peroxisome proliferator-activated receptor delta. *Cancer Cell* 2004;6:285–95. [PubMed: 15380519]

31. Sonoshita M, Takaku K, Sasaki N, et al. Acceleration of intestinal polyposis through prostaglandin receptor EP2 in Apc(Delta 716) knockout mice. *Nat Med* 2001;7:1048–51. [PubMed: 11533709]
32. Olmos G, Arenas MI, Bienes R, et al. 15-Deoxy-Delta(12,14)-prostaglandin-J(2) reveals a new pVHL-independent, lysosomal-dependent mechanism of HIF-1alpha degradation. *Cell Mol Life Sci* 2009;66:2167–80. [PubMed: 19458911]
33. Skuli N, Monferran S, Delmas C, et al. Activation of RhoB by hypoxia controls hypoxia-inducible factor-1alpha stabilization through glycogen synthase kinase-3 in U87 glioblastoma cells. *Cancer Res* 2006;66:482–9. [PubMed: 16397264]
34. Park JM, Kanaoka Y, Eguchi N, et al. Hematopoietic prostaglandin D synthase suppresses intestinal adenomas in ApcMin/+ mice. *Cancer Res* 2007;67:881–9. [PubMed: 17283118]
35. Kim WJ, Kim JH, Jang SK. Anti-inflammatory lipid mediator 15d-PGJ2 inhibits translation through inactivation of eIF4A. *Embo J* 2007;26:5020–32. [PubMed: 18034160]
36. Murakawa H, Bland CE, Willis WT, Dallman PR. Iron deficiency and neutrophil function: different rates of correction of the depressions in oxidative burst and myeloperoxidase activity after iron treatment. *Blood* 1987;69:1464–8. [PubMed: 3032307]
37. Fleming RE. Iron and inflammation: cross-talk between pathways regulating hepcidin. *J Mol Med* 2008;86:491–4. [PubMed: 18425494]
38. Pantopoulos K. Iron metabolism and the IRE/IRP regulatory system: an update. *Ann N Y Acad Sci* 2004;1012:1–13. [PubMed: 15105251]

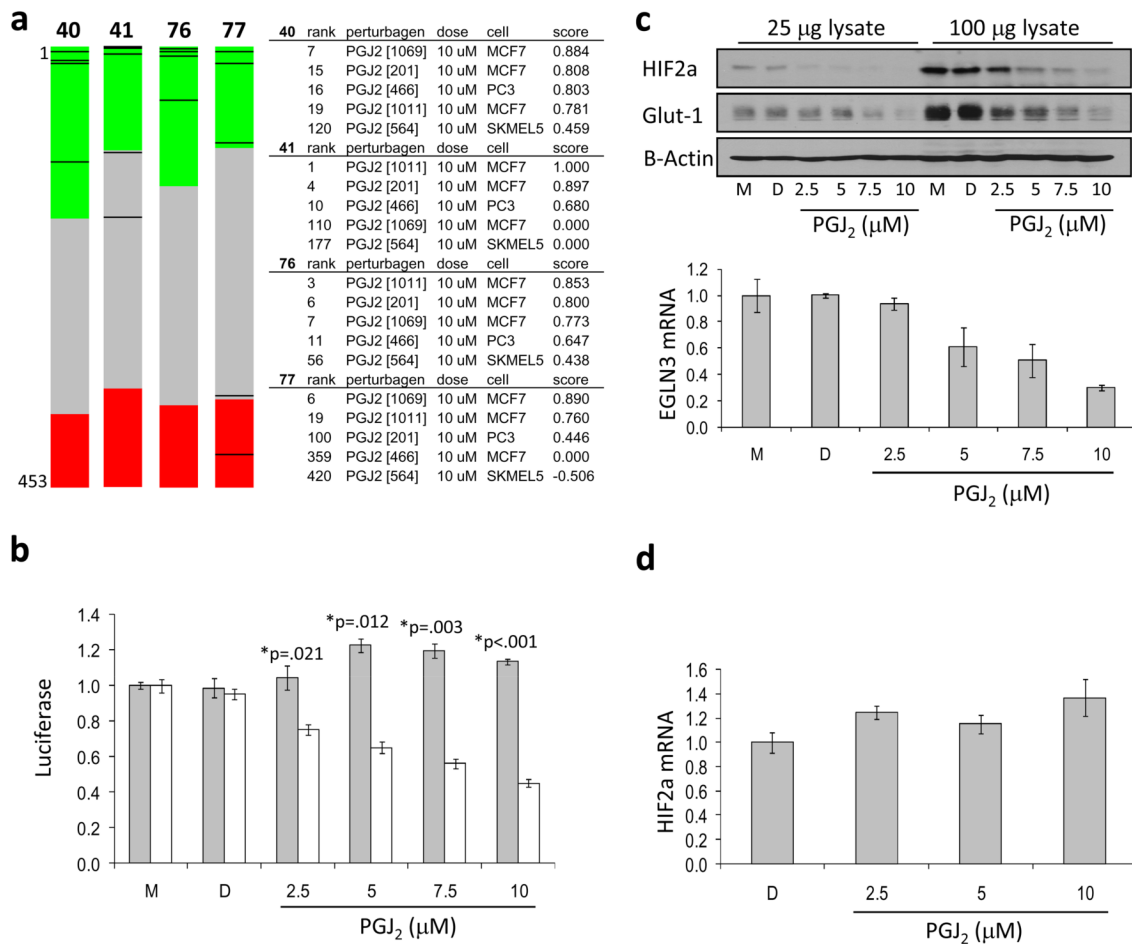


Figure 1. The Connectivity Map links inhibition of HIF activity to 15-deoxy- $\Delta^{12,14}$ -Prostaglandin J_2

(a) *Connectivity mapping of small molecule HIF2a inhibitors.* The ‘barview’ is constructed from 6,100 horizontal lines, each representing an individual treatment instance, ordered by their corresponding connectivity scores with signatures produced from compounds 40, 41, 76, and 77, as indicated (+1, top; 1, bottom). All PGJ₂ instances in the dataset ($n=15$) are colored in black bars (left). Colors applied to the remaining instances (i.e. gene expression profiles of the cells obtained with other than PGJ₂ compounds) reflect the sign of their scores (green, positive; gray, null; red, negative). The rank, name of the perturbagen [instance id], concentration, cell line and connectivity score for each PGJ₂ instance is also shown (right). Permutation p-values for the set of all PGJ₂ instances are <0.00001 for compounds 40, 41 and 76, and 0.01374 for compound 77. (b) *Effect PGJ₂ on HRE-luciferase reporter activity.* Stable 786-O cells harboring Hypoxia Response Element-driven luciferase reporter plasmid (7H4, white bars) or the hypoxia independent, SV40-driven luciferase reporter plasmid (7SV, gray bars), were treated with PGJ₂, DMSO as diluent control (D) or medium only (M). Relative luciferase activity was normalized to that of medium only treated cells, which was set to 1. (c) *Effect of PGJ₂ on HIF2a protein expression and HIF2a target gene expression.* 786-O cells were treated with the indicated concentrations of PGJ₂ as described in Materials and Methods. HIF2a and Glut-1 expression was analyzed by Western blot. B-Actin is shown as loading control (upper panels). EGLN3 expression was measured by quantitative reverse transcription polymerase chain reaction (qRT-PCR), normalized to beta-2-microglobulin (B2M) (lower panel). (d) *PGJ₂ does not affect HIF2a mRNA expression.* qRT-PCR was performed using

RNA extracted from 786-O cells treated in parallel with PGJ₂. Data shows relative expression of HIF2a message, normalized to beta-2-microglobulin (B2M). For all panels, error bars represent standard error of the mean (SEM).

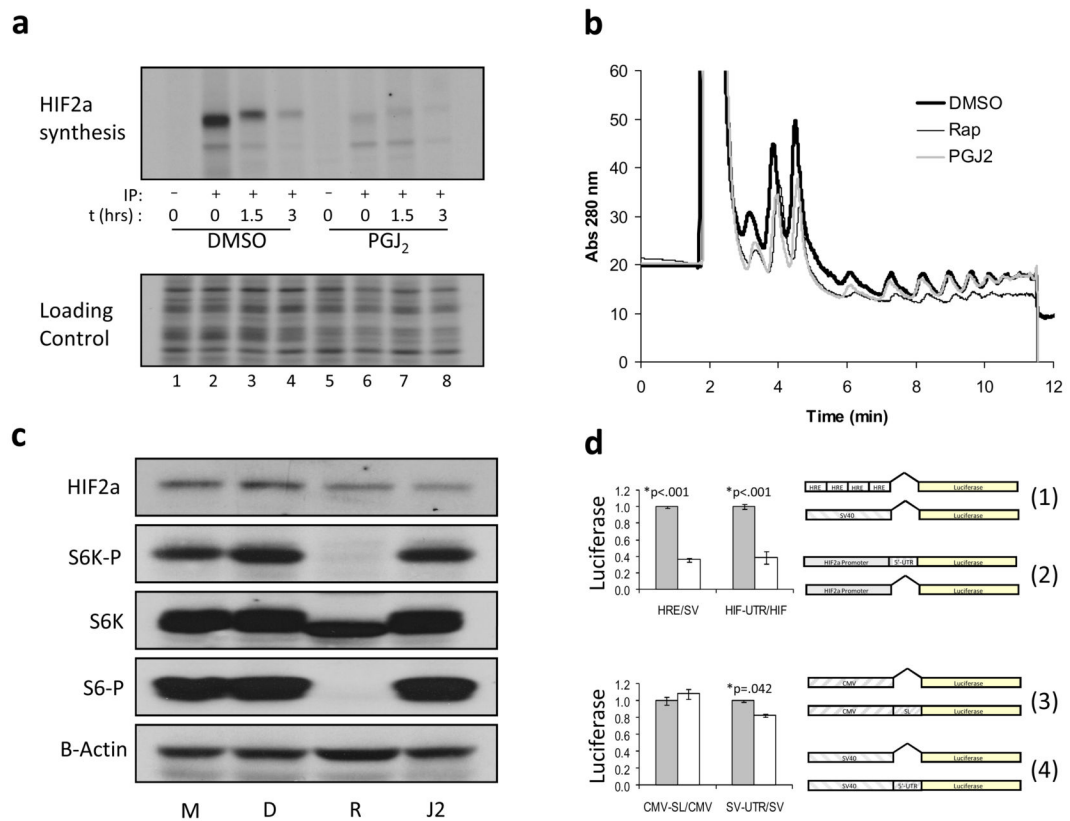
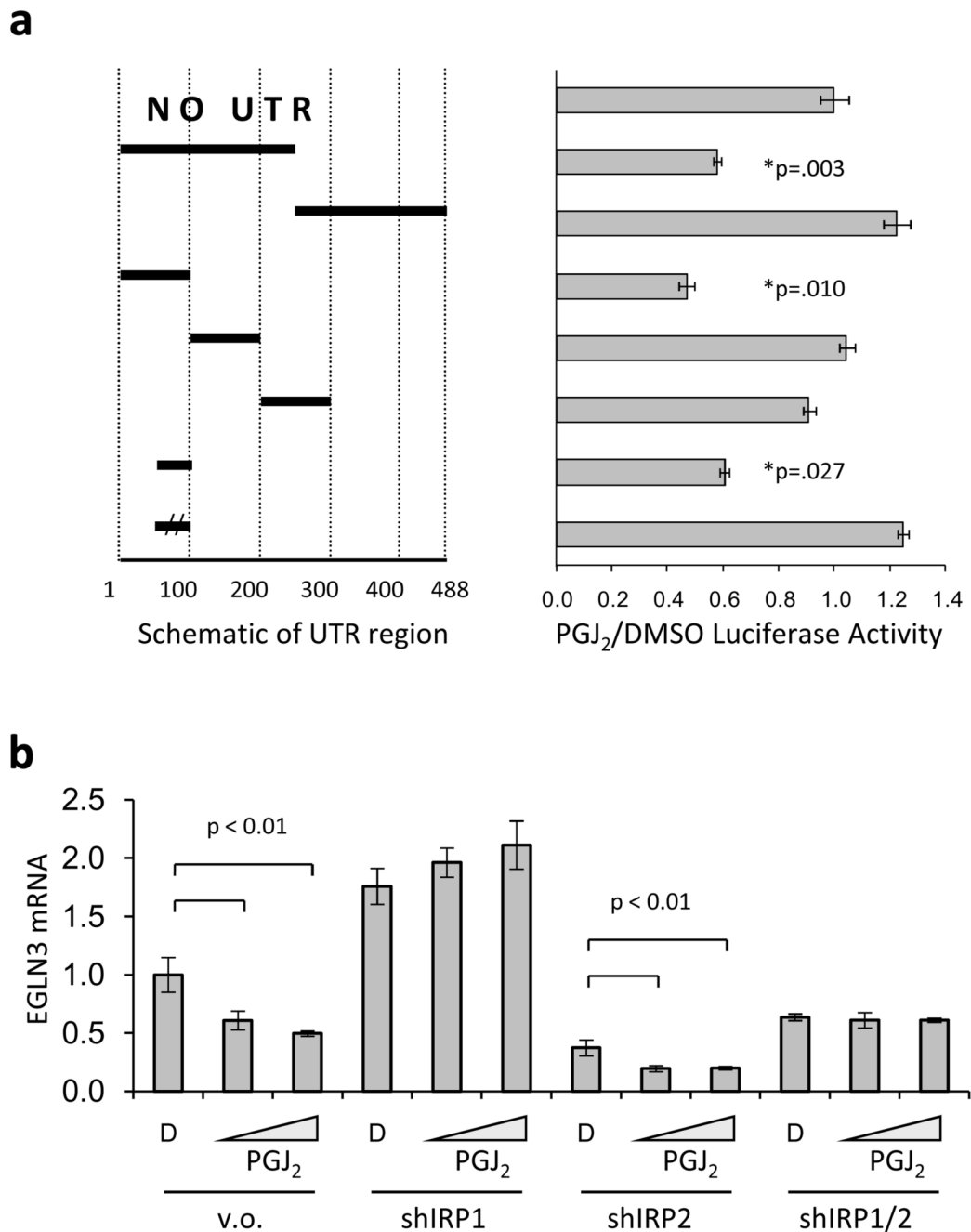


Figure 2. 15-deoxy- $\Delta^{12,14}$ -Prostaglandin J₂ decreases HIF2a mRNA translation in a HIF2a 5'-UTR-dependent manner

(a) ³⁵S-methionine pulse-chase analysis. 786-O cells were treated with 10 μ M PGJ₂ and subjected to ³⁵S-methionine pulse-chase immunoprecipitations (IP). Upper panel: autoradiography of HIF2a immunoprecipitations following the addition of excess cold methionine (chase) for the indicated time; (-) IP with control antibody (anti-HA), (+) IP with anti-HIF2a antibody. Lower panel: representative section of the autoradiograph in which a 1/1000th of the lysate used in the IP was directly loaded. Lanes 1–4, cells treated with DMSO only; lanes 5–8, cells treated with 10 μ M PGJ₂. (b) PGJ₂-treated cells exhibit a normal polysome profile. One of three independent experiments is shown. Thick black line, DMSO; thin black line, 50 nM rapamycin; gray line, 10 μ M PGJ₂. (c) Effect of PGJ₂ is mTOR independent. 786-O cells were treated with medium only (M), DMSO (D), 50 nM rapamycin (R), or 10 μ M PGJ₂ (J2). HIF2a, total p70S6K (indicated as S6K), phospho-T389 p70S6K (indicated as S6K-P), and phospho-S235/6 S6 (indicated as S6-P), expression was analyzed by Western blot. B-Actin is shown for loading control. (d) Effect of 15-deoxy- $\Delta^{12,14}$ -Prostaglandin J₂ is dependent upon the presence of the 5'-UTR and is heterologously transferable. Stable 786-O derived polyclonal cells expressing luciferase reporters were treated with DMSO only (gray bars) or 10 μ M PGJ₂ (white bars). Upper panel: comparison of ratios of (1) HRE/SV40 luciferase activities to that of (2) HIF2a promoter with the 5'-UTR divided by the HIF2a promoter alone. Lower panel: comparison of the ratios of (3) CMV-SL divided by CMV promoter alone to that of (4) SV40-UTR divided by SV40 promoter alone. Shown are p-values determined using the Student's unpaired homoscedastic t-Test with a two-tailed distribution. No significant differences were found in a likewise comparison of PGJ₂ versus DMSO treated CMV-SL divided by CMV promoter alone. All experiments were done in triplicate. Error bars represent standard error of the mean (SEM). Promoter-reporter constructs used in this analysis are diagrammatically presented to the right.



Western blot (data not shown). These cells were treated with PGJ₂ and EGLN3 mRNA expression was measured by qRT-PCR, normalized to beta-2-microglobulin (B2M). All measurements were done in triplicate and error bars represent standard error of the mean (SEM).

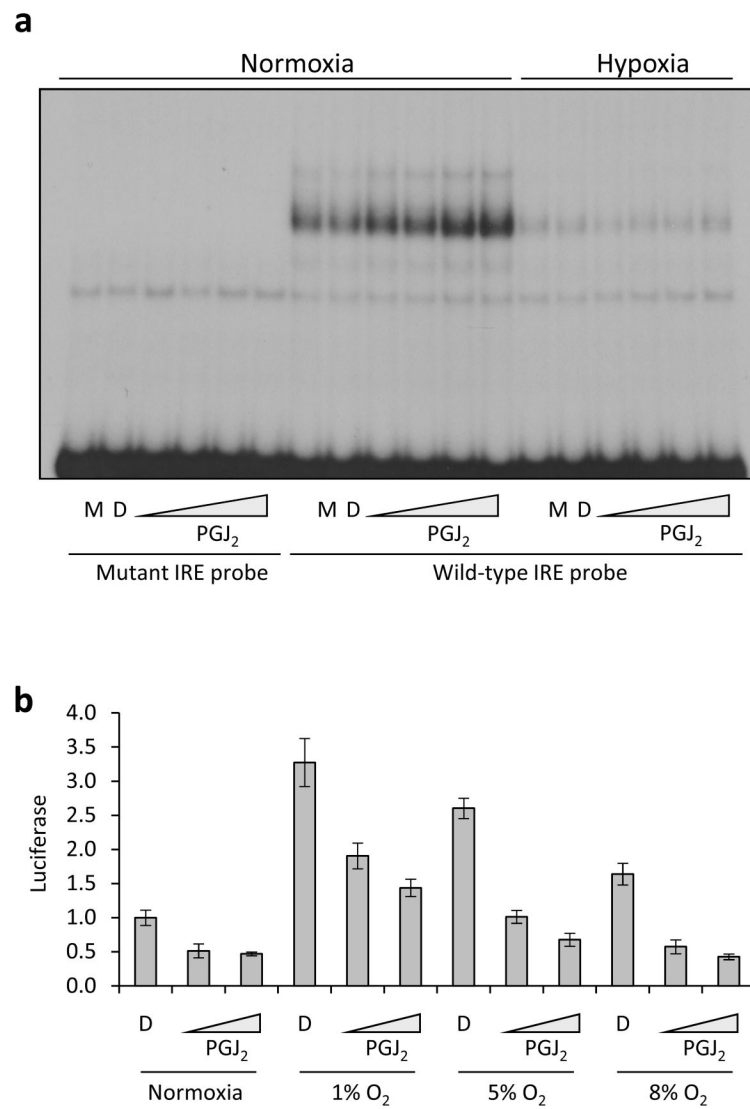


Figure 4. PGJ₂ promotes binding of IRP1 to HIF2a IRE under normoxic and hypoxic conditions
 (a) PGJ₂ promotes the binding of IRP1 to the HIF2a IRE. 786-O cells were treated with medium only (M), DMSO (D) or increasing concentrations of PGJ₂ at 21% ambient oxygen tension (normoxia) or 1% ambient oxygen tension (hypoxia), as indicated. (b) PGJ₂ represses HIF2a activity under normoxic and hypoxic conditions. 786-O cells harboring Hypoxia Response Element-driven or control SV40-luciferase reporter plasmid were treated with DMSO as diluent control (DMSO) or PGJ₂ at the indicated concentrations and cultured at a range of ambient oxygen tensions. All HRE divided by SV40 luciferase values are normalized to the DMSO control under normoxic conditions. Assay was done in triplicate and the error bars represent SEM.

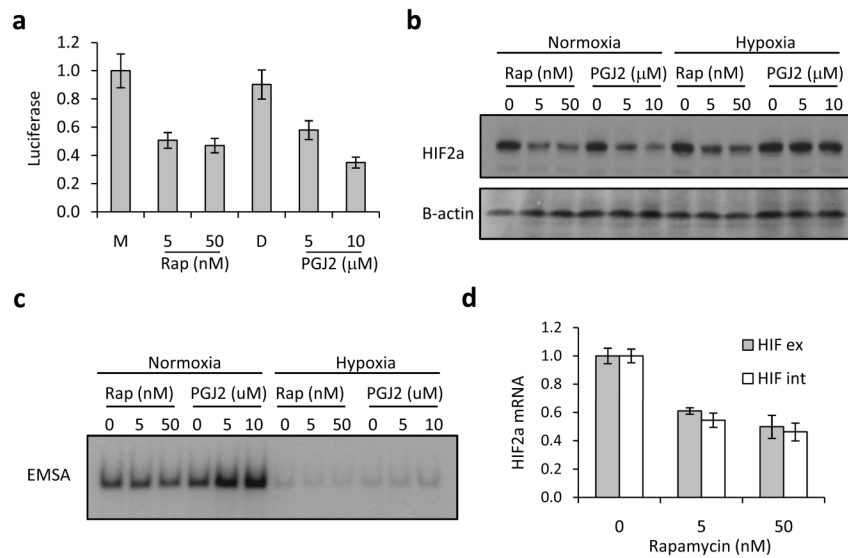


Figure 5. Rapamycin does not affect IRP1 binding to the HIF2a IRE

a) *Effect of Rapamycin versus PGJ₂ on HRE-luciferase activity.* Ratio of luciferase activity from HRE- over control SV40-reporter lines treated with Rapamycin or PGJ₂. b) *Effect of Rapamycin versus PGJ₂ on HIF2a protein expression.* Western blot showing HIF2a and B-actin (loading control) expression for 786-O cells that were plated in duplicate and treated with the indicated concentrations of Rapamycin or PGJ₂. c) *Effect of Rapamycin versus PGJ₂ on the binding of IRP1 to the HIF2a IRE.* EMSA using 786-O cells treated identically as above using with radiolabeled HIF2a IRE probe. d) *Effect of Rapamycin on HIF2a mRNA expression.* qRT-PCR showing native and processed HIF2a messages in Rapamycin treated 786-O cells.